Research Article

Received: 10 November 2018 Revised: 4 March 2019 Accepted article published: 27 March 2019 Published online in Wiley Online Library:

(wileyonlinelibrary.com) DOI 10.1002/pi.5817

Emulsifier-free reversible addition–fragmentation chain transfer emulsion polymerization of alkyl acrylates mediated by symmetrical trithiocarbonates based on poly(acrylic acid)

Natalia S Serkhacheva,[a] Nikolay I Prokopov,[a] Elena V Chernikova,[b*] Elena Y Kozhunova,[c] Inna O Lebedeva[d,e] and Oleg V Borisov[d,e*]

Abstract

Emulsifier-free batch emulsion polymerization of *n*-butyl acrylate and its semi-batch copolymerization with 2,2,3,3,4,4,5,5-octafluoropentyl acrylate and 2,2,3,4,4,4-hexafluorobutyl acrylate both mediated by poly(acrylic acid) containing the trithiocarbonate group in the chain was employed to produce amphiphilic triblock copolymers. The polymerization-induced self-assembly of these copolymers in aqueous media gave rise to spherical core–shell particles. Irrespective of the experimental conditions, the polymeric product was characterized by a bimodal molecular weight distribution. The apparent violation of the reversible addition–fragmentation chain transfer polymerization mechanism may be attributed to restricted accessibility of the trithiocarbonate group in the self-assembled block copolymers for propagating radicals that enter into the particle. Mean-field theoretical arguments were employed to explain the exclusively spherical morphology of the particles observed in the experiment.

Keywords: polymerization-induced self-assembly; reversible addition–fragmentation chain transfer; symmetrical trithiocarbonates; amphiphilic block copolymers; mean-field theory

INTRODUCTION

Block copolymers comprising blocks of homopolymers or copolymers of various chemical natures are capable of self-assembly in bulk or in selective solvents thus giving rise to the formation of nanostructures of various morphologies.[1] Among them, amphiphilic block copolymers attract special interest due to the wide potential of their applications in environmentally friendly processes and formulations, in pharmaceutical and personal care products etc.[2,3]

Traditionally, self-assembled nanostructures of amphiphilic block copolymers are produced by molecularly dispersing block copolymer in a common solvent followed by dialysis against a solvent selective for one of the blocks and poor for another one.[1] Alternatively, insolubility of one of the blocks can be triggered by varied external conditions, e.g. by varying temperature if one of the blocks is thermosensitive. The macromolecules self-assemble in polymeric micelles according to the model of close association above the critical micelle concentration. However, in many cases the polymeric micelles are characterized by low lability, i.e. changes of the aggregation number, the structure of the core or the shell is kinetically hindered, and this feature becomes more pronounced with increase in the length of the blocks and increase in the glass transition temperature of the lyophobic block.[4,5]

It is well known that AB block copolymers are capable of self-assembly giving rise to micelles of diverse morphologies (spherical, cylindrical) or to lamellar structures or polymersomes. AB diblock copolymers with lyophilic block A and lyophobic block B form a spherical morphology when the ratio of polymerization degrees of the blocks is $P_B/P_A \leq 1$.[6,7] An increase of the lyophobic block length to $P_B/P_A \gg 1$ makes micelles with

* *Correspondence to: EV Chernikova, Faculty of Chemistry, Lomonosov Moscow State University, Leninskie Gory, 1, bld. 3, Moscow, 119991, Russian Federation, E-mail: chernikova_elena@mail.ru; or OV Borisov, Institut des Sciences Analytiques et de Physico-Chimie pour l'Environnement et les Matériaux, F-64053, 2 av. P.Angot, Pau, France. E-mail: oleg.borisov@univ-pau.fr*

a *MIREA – Russian Technological University, Lomonosov Institute of Fine Chemical Technologies, pr. Vernadskogo, 86, Moscow, Russian Federation*

b *Faculty of Chemistry, Lomonosov Moscow State University, Lenin Hills, 1, bld. 3, Moscow, Russian Federation*

c *Faculty of Phisics, Lomonosov Moscow State University, Lenin Hills, 1, bld. 2, Moscow, Russian Federation*

d *Peter the Great St Petersburg Polytechnic University, Polytekhnicheskaya, 29, St.Petersburg, Russian Federation*

e *Institut des Sciences Analytiques et de Physico-Chimie pour l'Environnement et les Matériaux, 2 av. P. Angot Pau, France*

spherical morphology thermodynamically unfavorable and, as a result, worm-like micelles, lamellae or vesicles are found as equilibrium structures.[5,8,9] It is important to notice that the driving force for formation of non-spherical aggregates is gain in conformational entropy of the long core-forming blocks. Therefore, at equilibrium non-spherical micelles are formed only by block copolymers with essentially asymmetric composition, i.e. with longer hydrophobic blocks. In such micelles the thickness of the corona is smaller than the radius of the core (so-called crew-cut aggregates).[10,11] For block copolymers with $P_B/P_A \gg 1$ fine tuning of the aggregate morphology is possible also by slight change of the environmental conditions (pH, ionic strength, composition of solvent, concentration of block copolymer etc.).[12]

Recently a versatile approach to producing amphiphilic block copolymers capable of self-assembly into nano-sized core–shell particles directly in the course of synthesis was developed. This approach is known as polymerization-induced self-assembly (PISA).[13–17] The main idea of PISA has been described in detail in numerous reviews and is based on the above-mentioned ability of amphiphilic block copolymers to self-assemble in a solvent which is good for one of the blocks and poor for another provided that the poorly soluble block is long enough.[18,19] Usually, polymerization of the monomers comprising the associating block is performed in the presence of a living polymer in a solvent which is thermodynamically good for the living polymer and poor for the growing polymer. The living polymer is chain-extended and the growing block of the polymerized monomer progressively loses its solubility. As a result, the self-assembly of the formed block copolymer into aggregatively stable particles occurs and further growth of the solvophobic block continues inside the particles. Thus, the living polymer performs two functions: it initiates the growth of the block copolymer and stabilizes the formed polymeric particles.

Depending on the solubility of the monomers in the reaction medium, PISA formulations include dispersion and emulsion polymerization, while the mechanism of formation of the block copolymer is usually based on the various types of reversible deactivation radical polymerization.[20–22] Reversible addition–fragmentation chain transfer (RAFT) polymerization is most frequently used because of its versatility and tolerance to a wide range of monomers and solvents.[23–26] RAFT dispersion polymerization, which starts from homogeneous conditions, is known to produce various morphologies of particles even within the same polymerization system if the synthesis conditions are varied.[27] In contrast, emulsifier-free RAFT emulsion polymerization usually results in the formation of core–shell particles with spherical morphology.[28] However, recently significant progress was achieved in extending the spectrum of morphologies formed in emulsion polymerization.[19]

RAFT formulations are based typically on monofunctional RAFT agents, e.g. dithiobenzoates or non-symmetrical trithiocarbonates that give rise to AB block copolymers. The progress achieved in PISA of AB block copolymers mediated by monofunctional RAFT agents was summarized in recent reviews.[13–15] In contrast, bifunctional RAFT agents, e.g. symmetrical trithiocarbonates that enable the synthesis of ABA triblock copolymers, have attracted much less attention. In our previous studies of emulsion homopolymerization and copolymerization of *n*-butyl acrylate (BA) in the presence of poly(acrylic acid) (PAA) based macroRAFT agents containing the trithiocarbonate group within the chain, we have analyzed the influence of monomer(s) to the medium volume ratio, the polymerization degree and the chemical nature of the co-monomer in the macroRAFT agent on polymerization kinetics, particle size and morphology, and the molecular weight distribution (MWD) of the polymerization products.[29–32]

Dispersion polymerization of acrylates mediated by symmetric hydrophilic or amphiphilic polymeric trithiocarbonates of general structure A–S–C(=S)–S–A usually provides relatively good control of the MWD. However, this control is lost at high conversions and, as a result, high molecular weight polymer is produced and the MWD gets broader. In these systems, independently of the polymerization conditions, i.e. the monomer to solvent ratio and the concentrations of macroRAFT agent and initiator (the former determines the ratio of A and B block lengths), particles of spherical morphology are formed.[31,32]

In contrast, emulsifier-free emulsion polymerization of acrylates mediated by the same macroRAFT agents A–S–C(=S)–S–A, based on for example PAA trithiocarbonate, leads to different results.[29–32] In contrast to products of solution or dispersion polymerization, the products of emulsion polymerization are typically characterized by a bimodal MWD in a wide range of monomer conversion. Moreover, in all cases the formation of particles of spherical morphology was observed.

The bimodal MWD was also described previously by Chenal *et al.*[33] for emulsifier-free emulsion polymerization of BA and by Chaduc *et al.*[34] for styrene polymerization, both mediated by PAA with a terminal trithiocarbonate group with attached dodecyl or propyl substituent. However, in the latter systems the evolution of the MWD depends on pH and monomer nature: at alkaline pH the locus of oligomeric mode on SEC traces remains constant throughout polymerization, while at acidic pH it first shifts to the higher molecular weight region and then remains constant. This effect is more pronounced in styrene polymerization.[34] The formation of the high molecular weight product is accompanied by slow consumption of the oligomeric one. Chenal *et al.*[33] ascribe this phenomenon to the low chain transfer coefficient of the macroRAFT agent. However, this interpretation disagrees with the higher efficiency of the same macroRAFT agent in solution and dispersion polymerization. The formation of an oligomeric product with molecular weight higher than the molecular weight of the macroRAFT agent also remains unexplained.

The kinetic features of BA emulsion polymerization mediated by a macroRAFT agent with a similar nature of a leaving polymeric substituent, PAA, but a different locus of the trithiocarbonate group in the chain are also different.[30,33] In particular, the induction period on the kinetic curves is longer, the number-average particle diameter is smaller and the rate of consumption of macroRAFT agent upon increasing monomer conversion is higher in the case of PAA with terminal trithiocarbonate group.[33]

Based on our previous results and literature data, we decided to look more deeply at the experimental conditions that lead to the bimodal MWD of polymers and the spherical morphology of the polymeric particles in emulsifier-free emulsion polymerization of alkyl acrylates in the presence of PAA with trithiocarbonate group located within the chain.

In particular, we systematically varied the conditions of emulsifier-free emulsion (co)polymerization of BA mediated by PAA trithiocarbonate and analyzed the MWD of the polymerization products as well as the average diameter of the formed particles and, in some cases, their morphology. We also suggest an explanation for our experimental observations in terms of the morphology of the resulting nanoparticles and support it by mean-field theoretical arguments.

In addition to the emulsion batch polymerization of BA, in the present study we performed semi-batch emulsion copolymerization of BA with fluoroalkyl acrylates. The choice of fluoroalkyl acrylates is primarily explained by the presence of a long fluoroalkyl group, which provides the low glass transition temperature of the polymer and its high hydrophobicity. The latter property may be particularly useful for coating applications. Previously, we have examined the batch copolymerization of these monomers and have discovered its general features.[31]

EXPERIMENTAL

Materials and polymer synthesis

Directly before use, the monomers acrylic acid, BA, 2,2,3,3,4,4,5,5-octafluoropentyl acrylate (OFPA) and 2,2,3,4,4,4-hexafluorobutyl acrylate (HFBA) and the solvents 1,4-dioxane and *N*,*N*-dimethyl formamide (DMF) were distilled. Initiators azo-bis-isobutyronitrile (AIBN) and 4,4′-azo-bis-cyanopentanoic acid were recrystallized from methanol and dried in vacuum; potassium persulfate (PSK) (ACS reagent, Aldrich) was used without further purification. The RAFT agent dibenzyl trithiocarbonate (BTC) was synthesized and characterized as described elsewhere.[35]

For the synthesis of PAA trithiocarbonate (PAATC), 1.45 g of BTC and 0.082 g of AIBN were dissolved in 25 mL of 1,4-dioxane. Then 25 mL of acrylic acid was added to this solution up to an equal volume ratio of the monomer and solvent. The final concentration of BTC in the reaction mixture was 0.1 mol L^{-1} and that of AIBN 1×10^{-3} mol L^{-1}. The reaction mixture was poured into an ampoule, degassed by repeating three freeze–evacuate–thaw cycles and sealed under vacuum. After heating at 80 °C for 24 h, the reaction mixture was cooled, then diluted with 1,4-dioxane and subjected to dialysis against water. The polymer was lyophilized from the water solution. According to SEC, $M_n = 4600$, $Đ = 1.24$.

Emulsifier-free emulsion polymerization of alkyl acrylates was conducted in batch and semi-batch regimes in a glass reactor equipped with a water jacket, stirrer and condenser in a nitrogen atmosphere on stirring (300 rpm) at 70 °C. The volume ratios of the monomer to aqueous phase were equal to 1:10.

In a general procedure, a macroRAFT agent (10 wt% to monomer) was dissolved in bidistilled water. After that the pH was adjusted to 5.4. BA was added to the aqueous solution. The reactor with the prepared solution was purged with nitrogen for 30 min with stirring (300 rpm). Then the required amount of the initiator aqueous solution was added to the reactor (in the case of AIBN, it was added with monomer) and the system was purged with nitrogen again. In the case of the semi-batch regime, OFPA or HFBA was added dropwise a definite period after the start of BA polymerization; the molar ratio of BA and fluoroalkyl acrylate was 4:1. At required periods the samples were taken for analysis.

A typical recipe includes 0.8935 g of PAATC as the macroRAFT agent, 100 mL of bidistilled water as the continuous phase, 8.935 (10 mL) of BA and 0.111 g of PSK as the initiator. In the semi-batch regime, for example, 7.151 g (8 mL) of BA and 3.977 g (2.7 mL) of OFPA are used.

The total monomer conversion was determined by gravimetry taking into account the weight of PAATC in the probe.

To estimate the locus of the trithiocarbonate group in the macromolecules, the polymer solution (1 wt%) in DMF was subjected to methylation by diazomethane. After methylation was completed, 5 mL of the methylated polymer solution was added to AIBN (0.1 mol L^{-1}). Then the solution was degassed and the ampoule was sealed and immersed in a water bath pre-heated at 80 °C for 24 h. The polymer solution was cooled and analyzed by SEC.

Instrumentation

The average molecular weights and dispersity ($Đ = M_w/M_n$) were determined by SEC. The SEC measurements were performed in DMF containing 0.1 wt% LiBr at 50 °C with a flow rate of 1.0 mL min^{-1} using a chromatograph GPC-120 PolymerLabs equipped with refractive index detector and with two columns PLgel 5 μm MIXED B for the molecular weight range $5 \times 10^2 - 1 \times 10^7$. The SEC system was calibrated using narrow dispersed linear poly(methyl methacrylate) standards with molecular weight ranging from 800 to 2×10^6 g mol^{-1}. A second-order polynomial was used to fit the $\log_{10} M$ *versus* retention time dependence. All polymers containing units of acrylic acid were subjected to methylation by diazomethane before analysis.

The average diameter of particles of the polymeric dispersions was determined by dynamic light scattering (DLS) using a photon analyzer Zetasizer Nano-ZS Malvern equipped with a He–Ne laser as a light source ($\lambda = 633$ nm and light source power 5 mW) with a measurement range of particle sizes from 0.6 to 6000 nm. The initial dispersions were diluted with bidistilled water and dedusted by filtration. The measurements were conducted at room temperature with a scattering angle of 173° in the automatic mode according to the standard procedure.

Microphotographs of the dispersions were obtained using a Leo 912 AB Omega (Karl Zeiss) transmission electron microscope operating at an accelerating voltage of 100 kV; 1 μL drops of the diluted emulsion solutions were deposited on carbon-coated copper TEM grids and dried at room temperature.

The absorption spectra of the polymers (1 mg mL^{-1}) were recorded in tetrahydrofuran at room temperature on a Unico 2804 UV–visible spectrometer (USA).

RESULTS AND DISCUSSION

Emulsifier-free emulsion homopolymerization and copolymerization of *n*-butyl acrylate mediated by poly(acrylic acid) with trithiocarbonate group in the chain

Chain extension of a hydrophilic or amphiphilic (co)polymer with the trithiocarbonate group in the chain by hydrophobic monomer B proceeds via a complicated mechanism. The reaction between the propagating hydrophobic oligoradical B• and the macroRAFT agent A–SC(=S)S–A located in the aqueous phase results in the formation of the amphiphilic diblock copolymer A–SC(=S)S–B and release of the macroradical A• capable of initiating polymerization of monomer B:

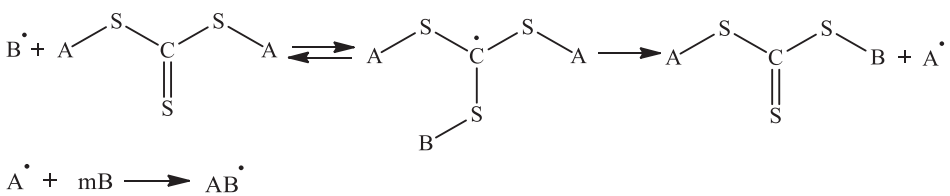

where A is PAA and B is BA, HFBA and OFPA. The further determination of the process is determined by the length of the oligoradical B• attached to the macroRAFT agent. In turn, this length of the oligoradical depends on, besides other conditions, the concentrations of macroRAFT agent and monomer.

Diblock copolymers may continue to participate in the reversible chain transfer reactions (see below) in the case of a relatively short hydrophobic block and/or a low copolymer concentration in the solution that prevents formation of micelles.

However, according to our previous data, the insertion of several units of alkyl acrylate into the PAA chain results in enhancing the surface active properties of the polymer.[29–32] After reaching the critical micelle concentration, which is typically below 0.1 wt%[32] (it corresponds to *ca* 1% conversion of polymeric RAFT agent), the amphiphilic block copolymers form micelles. The incorporation of A• or AB• oligoradical into the micellar core, which may also contain a certain amount of hydrophobic monomers, launches the nucleation of the polymeric particles and the sequence of reversible chain transfer reactions:

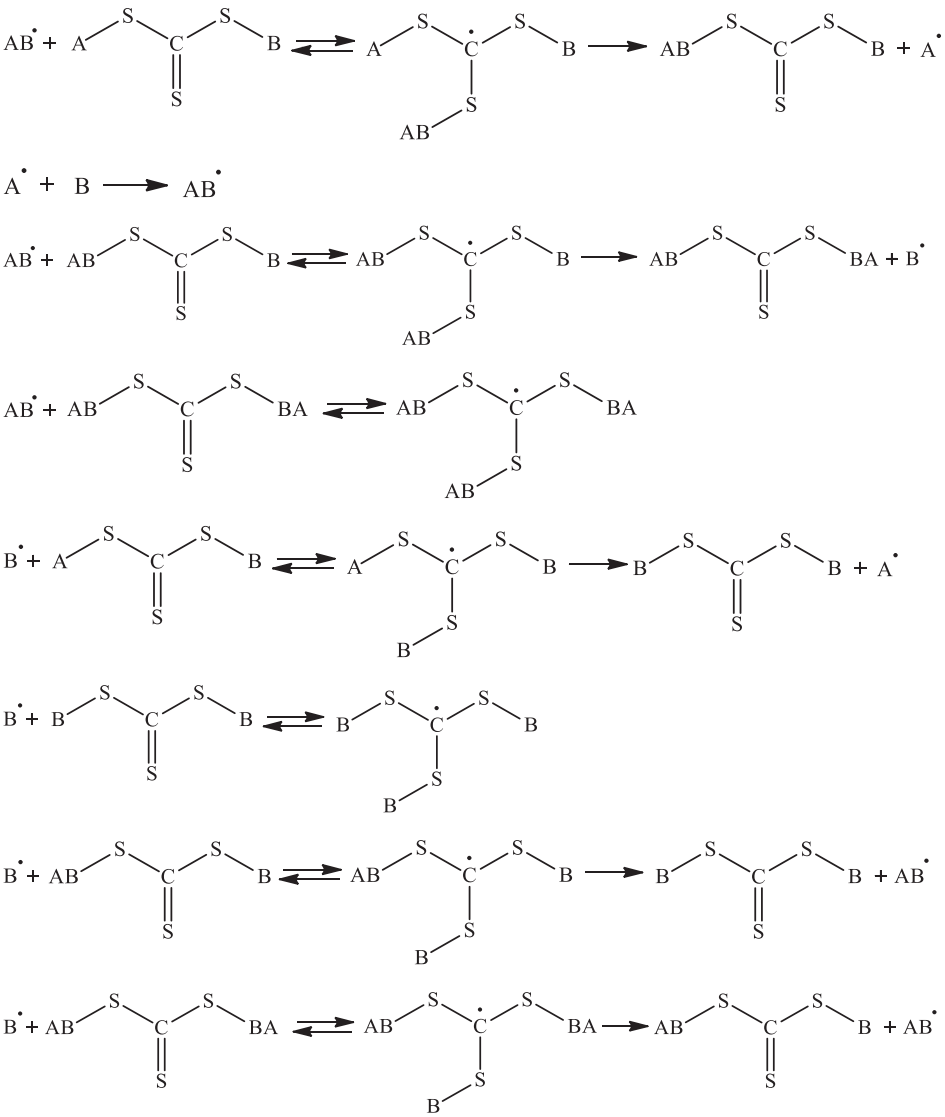

In the ideal case, this sequence will lead to the formation of triblock copolymer AB–SC(=S)S–BA and a certain amount of homopolymer B–SC(=S)S–B. However, deviation from this mechanism, e.g. desorption of intermediate products from the micelles or particles and the termination reactions of radical species (propagating radicals, intermediate radicals), may cause also the formation of 'dead' chains.

Batch emulsion polymerization

As mentioned above, the typical feature of acrylate emulsion homopolymerization and copolymerization in the presence of a hydrophilic or amphiphilic macroRAFT agent based on symmetric trithiocarbonate is a bimodal MWD of the products. At the same time, unlike *ab initio* emulsion polymerization, both dispersion and solution polymerizations of BA mediated by PAATC resulted in unimodal MWD.[29,31] We suppose that the low molecular weight fraction corresponds to the block copolymer with a short hydrophobic block formed during stage I of the emulsion batch polymerization, while the high molecular weight mode can be attributed to

further grown polymer. This is a debatable statement. Therefore, we have studied this process again in both batch and semi-batch regimes searching for the conditions that enable us to minimize the oligomeric fraction. In the case of the batch regime, our studies of BA emulsion polymerization initiated by PSK and mediated by PAATC were supplemented by additional investigations of the influence of the PSK and PAATC concentrations on the kinetics and MWD of the products. The range of concentrations was chosen on the basis of our previous results.[30,31]

Figure 1 illustrates the kinetics of emulsifier-free emulsion polymerization of BA initiated by PSK in the presence of PAATC with various concentrations of PAATC (Fig. 1(a)) and PSK (Fig. 1(b)) at a water to monomer volume ratio equal to 10. The S-shaped profile of the kinetic curves is typical for emulsion polymerization. The induction period corresponding to stage I of the emulsion polymerization is not influenced by PAATC concentration, but it is shortened with an increase in the PSK concentration. The length of the growing block naturally shortens with an increase in the PAATC concentration. However, under chosen conditions (10–20 wt% of PAATC corresponding to $[PAATC] = (1.8–3.6) \times 10^{-3}$ mol L^{-1}) the formation of a hydrophobic block of critical length should occur at very low monomer conversion, i.e. after a short polymerization time, which results in a similar induction period. In contrast, PSK provides an increase in the number of initiating radicals and even a minor decrease in the initiator concentration results in slowing down the nucleation of the particles. In general, both an increase in PAATC and a decrease in PSK result in diminution of the polymerization rate, and therefore a bigger molar ratio $[PSK]/[PAATC] \geq 1$ is required to achieve monomer conversion above 90%.

The number-average hydrodynamic diameter (D_n) of the particles, as determined by DLS, is slightly affected by PAATC concentration (Fig. 2(a)). After the end of stage I, D_n either remains constant or grows during the main process of polymerization. The final value of D_n slightly decreases with increase of PAATC content from 10 to 15 wt% and then it grows at 20 wt% of PAATC. In contrast, the value of D_n is practically independent of PSK concentration (Fig. 2(b)).

A similar transformation of the MWD of the polymers formed in the course of polymerization was discovered irrespective of the polymerization conditions used. As can be seen from Fig. 3 (curves 1–3), a slight shift of the chromatogram to the high molecular weight region is observed in the initial stages of polymerization (during the induction period) for the system described in Fig. 1(b) (curve 3). The end of the induction period is followed by the formation of a high molecular weight product and transformation of the MWD shape from unimodal to bimodal (Fig. 3, curve 4). In contrast to the data presented by Chenal *et al.*[33] where shorter PAA was used with a hydrophobic terminal $-SC(=S)S-C_{12}H_{25}$ group, PAATC with the $-SC(=S)S-$ group in the chain is rapidly chain-extended which leads to the formation of block copolymers with a short hydrophobic block. The slight change in molecular weight and the number of possible reactions resulting in a change of the locus of the $-SC(=S)S-$ group in the chain make difficult a reliable estimation of the exact structure of block copolymers formed at this stage by aminolysis[36] or by performing the reaction with excess of initiator.[37]

Nevertheless, we tried to estimate the locus of the trithiocarbonate group in the product formed during the induction period. In order to do this, we performed the reaction of the polymer formed after 5 min of polymerization with an excess of initiator using the procedure described by Chernikova *et al.*[37] If the structure of the formed macromolecules is $P_nSC(=S)SP_m$, then upon heating with excess of radical initiator a consequent cleavage of polymeric substituents from the macromolecule should occur and the released macroradicals should be terminated by the initiator radicals. This reaction leads to the formation of new macromolecules with lower molecular weight compared to that of the initial macromolecules. Figure 4 presents the SEC traces of the product of emulsion polymerization formed after 5 min during the induction period (curve 1), and the same polymer after heating at 80 °C in the presence of 100-fold excess of AIBN (curve 2). The chromatogram of the polymer after its thermal treatment with AIBN has shifted to the low molar mass region indicating the locus of the trithiocarbonate group inside the chain. The set of columns used in SEC does not allow us to detect low molar mass products; however, they can separate effectively macromolecules with molecular weight larger than 10^3 g mol^{-1}.

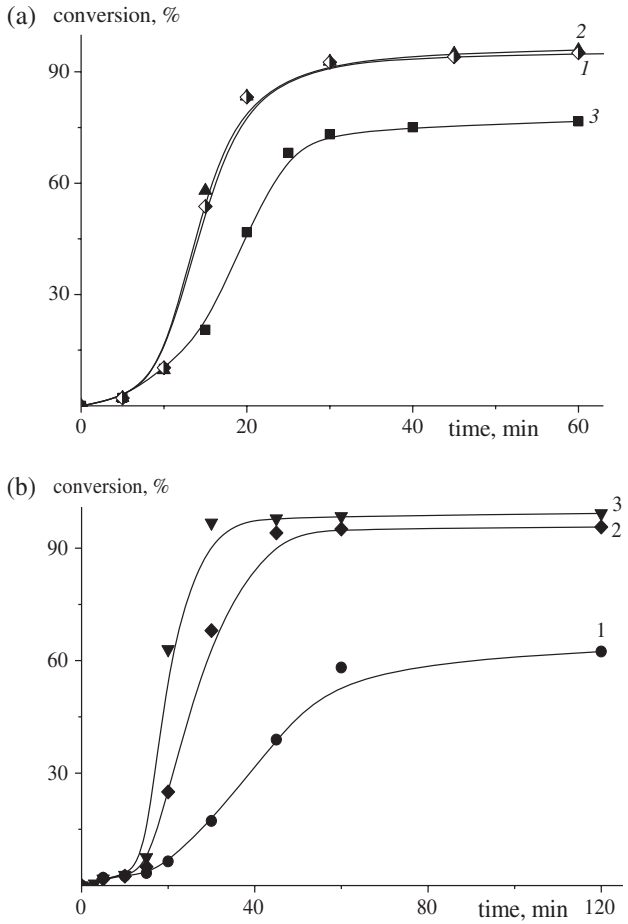

Figure 1. Dependence of monomer conversion on the reaction time for the batch emulsion polymerization of BA at 70 °C in the presence of PAATC; water:monomer = 10:1 v/v, pH 5.4: (a) 0.9 wt% of PSK, PAATC 10 wt% (curve 1), 15 wt% (curve 2) and 20 wt% (curve 3); (b) 10 wt% PAATC, PSK 0.75 wt% (curve 1), 0.9 wt% (curve 2) and 1.0 wt% (curve 3).

Incorporation of BA units in the PAA chain can be confirmed independently by a slight change of the glass transition temperature from 120 °C for PAATC to 99 °C for the product formed after 5 min of polymerization (1.8% of monomer conversion).

Finally, we confirmed that macromolecules formed during the induction period and just after its completion keep their thiocarbonyl functionality. The products formed after 3, 5 and 15 min of polymerization (Fig. 3, curves 1, 2 and 4) were dissolved in tetrahydrofuran (1 mg mL^{-1}) and analyzed by UV–visible spectroscopy

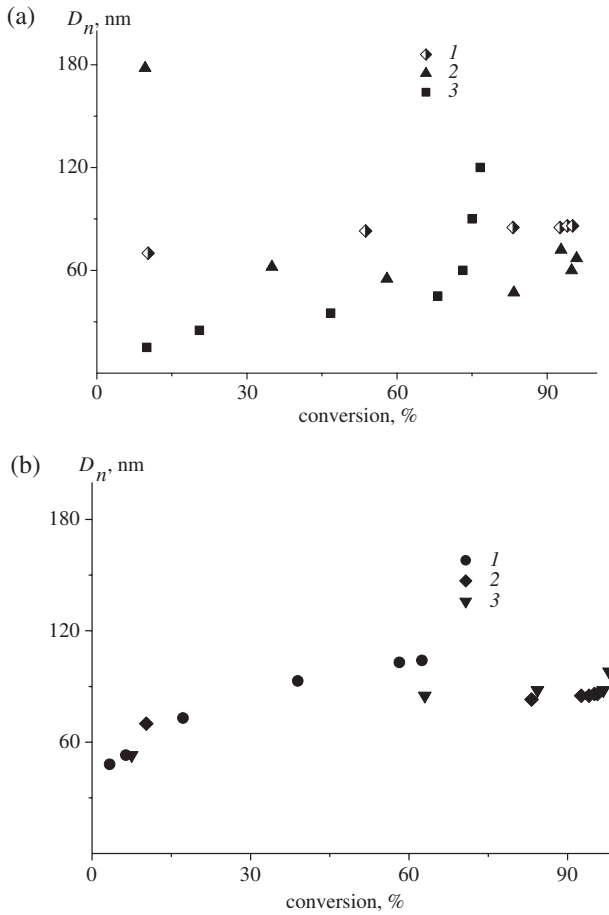

Figure 2. Dependence of the number-average diameter D_n of the particles on polymerization time for the batch emulsion polymerization of BA at 70 °C in the presence of PAATC; water:monomer = 10:1 v/v, pH 5.4: (a) 0.9 wt% of PSK, PAATC 10 wt% (points 1), 15 wt% (points 2) and 20 wt% (points 3); (b) 10 wt% PAATC, PSK 0.75 wt% (points 1), 0.9 wt% (points 2) and 1.0 wt% (points 3).

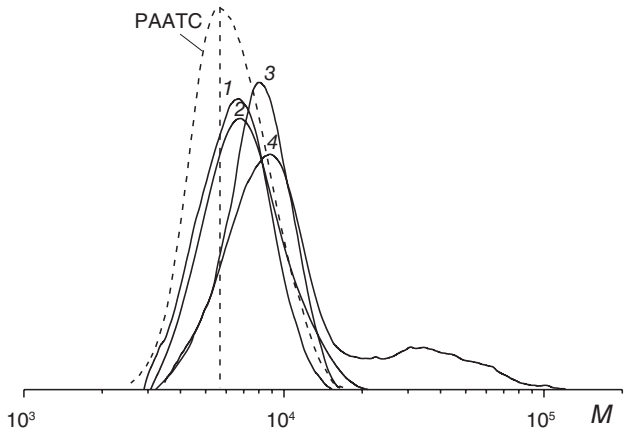

Figure 3. SEC curves normalized to unit area for polymers formed at various monomer conversions during the batch emulsion polymerization of BA at 70 °C mediated by 10 wt% PAATC, 1 wt% of PSK, water:monomer = 10:1 v/v, after 3 min (curve 1), 5 min (curve 2), 10 min (curve 3) and 15 min (curve 4) of polymerization.

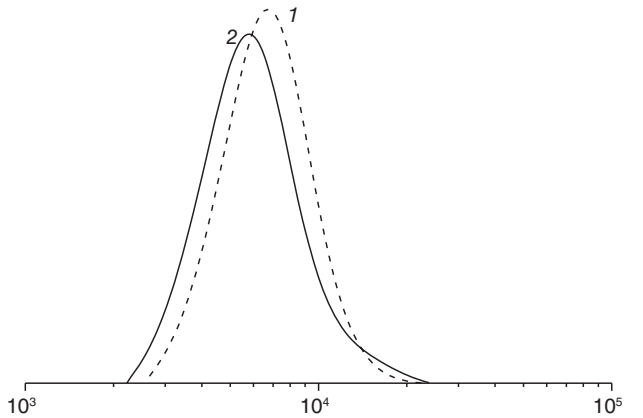

Figure 4. SEC curves normalized to unit area for the product of emulsion polymerization formed during the induction period (curve 1) and the same polymer after heating with 0.1 mol L^{-1} AIBN in DMF solution at 80 °C for 24 h (curve 2).

(Fig. 5). Figure 5 illustrates the absorption spectra of the polymers taken at the same weight concentration. As seen from the UV–visible spectra, an intense maximum at 305–307 nm which corresponds to absorption of the trithiocarbonate group[37] is observed. The absorption maximum intensity slightly decreases upon increase of the polymerization time. However, this decrease is caused by an increase of the molecular weight of the polymer and hence a decrease of the concentration of the chains in a probe of the same weight. Thus, the amount of chains formed during the induction period and containing trithiocarbonate groups remains approximately constant.

Hence, after completion of the induction period the newly formed product is slowly consumed; simultaneously a product with higher molecular weight is formed, i.e. the MWD becomes bimodal (Fig. 6).

Upon progress in the monomer conversion, the molecular weight of the high molecular weight product increases. Evidently, the slow consumption of the oligomeric block copolymer cannot be explained by its low efficiency in polymerization from a chemical standpoint. First, it exhibits high efficiency in dispersion and solution polymerizations.[29,31] Moreover, in the structure of the intermediate radical which is formed after addition of the propagating radical to the C=S bond of the block copolymer with the trithiocarbonate group, the chemical nature of all the monomer units attached to sulfur atoms of the trithiocarbonate group of the intermediate product is the same. Hence, fragmentation of the intermediate product should result in the revival of macroradicals capable of further propagation. At the same time, one could hypothesize that, in the case of the block copolymer with a short hydrophobic block based on symmetrical trithiocarbonate, the trithiocarbonate group is located close to the interface of the particle. Upon progress in the monomer conversion, a fraction of these groups is hidden from the propagating radicals and is excluded from participation in the reversible chain transfer reactions. As a result, the molar concentration of the growing chains decreases and control of the MWD may worsen. Variation of the PSK or PAATC concentrations has practically no visible effect on the ratio between the oligomeric and polymeric fractions.

However, analysis of the number-average molecular weight M_n of the high molecular weight product shows that M_n grows in the course of polymerization to limiting high conversions. This observation implies that the high molecular weight polymeric product is living (Fig. 7).

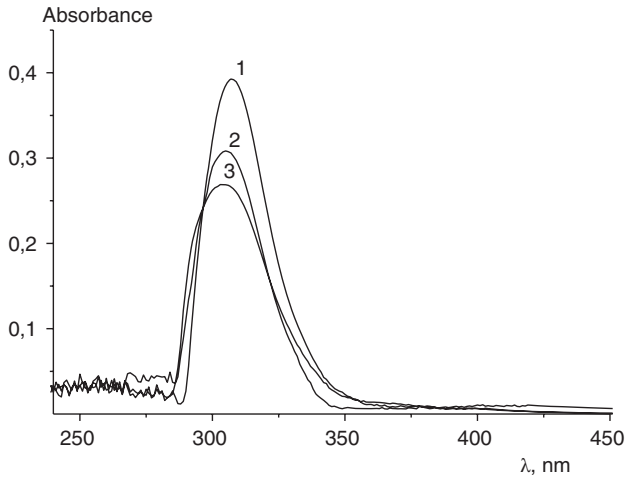

Figure 5. UV–visible spectra of the products of the batch emulsion polymerization of BA at 70 °C mediated by 10 wt% PAATC, 1 wt% PSK, water:monomer = 10:1 v/v, after 3 min (curve 1), 5 min (curve 2) and 15 min (curve 3) of polymerization.

This product is characterized by a low dispersity $Đ = M_w/M_n$ up to about 30% of monomer conversion. The simultaneous deviation from linear dependence of M_n *versus* conversion observed at intermediate conversions correlates with an increase in dispersity and indicates violation of the RAFT mechanism. These features are probably related to the chosen molar ratio [PSK]/[PAATC] ≥ 1, which typically results in the simultaneous formation of living and dead macromolecules. In this case, estimation of the locus of the trithiocarbonate group in the macromolecules formed at high monomer conversion becomes too rough due to the coexistence of both living and dead polymer chains in the product.

Even in the case when dispersions of the particles obtained after polymerization comprise two fractions of macromolecules with different molecular weights and do not contain any additional stabilizer, the particles keep their aggregative stability for at least several weeks. Analysis of the morphology of their thin films by TEM reveals the formation of spherical particles; a typical micrograph is presented in Fig. 8.

Semi-batch emulsion polymerization

The semi-batch regime was applied to emulsion copolymerization of BA with fluoroalkyl acrylates (HFBA and OFPA) mediated by PAATC. As we have shown previously, the batch regime results in a prolonged induction period and slow kinetics for these systems compared to BA homopolymerization under similar conditions. Moreover, copolymerization of BA and OFPA is strongly retarded.[31] The dropwise addition of fluoroalkyl acrylate in 10 min after the start of the BA polymerization accelerates the polymerization kinetics (Fig. 9(a), curves 1 and 2). However, an increase of the hydrophobicity of fluoroalkyl acrylate, i.e. replacement of HFBA by OFPA, results in a reduction of the polymerization rate (Fig. 9(a), curves 2 and 3). In this case, an increase in the initiator concentration improves the polymerization kinetics (Fig. 9(b)).

Before addition of fluoroalkyl acrylates, the average value of D_n of the already formed particles in the studied systems was about 65 nm. After addition of fluoroalkyl acrylates, the value of D_n grows progressively in the course of polymerization (Fig. 7). An increase in hydrophobicity of the co-monomer leads to a slight decrease in the value of D_n for the final dispersions: 138 nm for HFBA and 111 nm for OFPA (Fig. 10(a)). A change in PSK concentration has no visible effect on the average size of the particles (Fig. 10(b)).

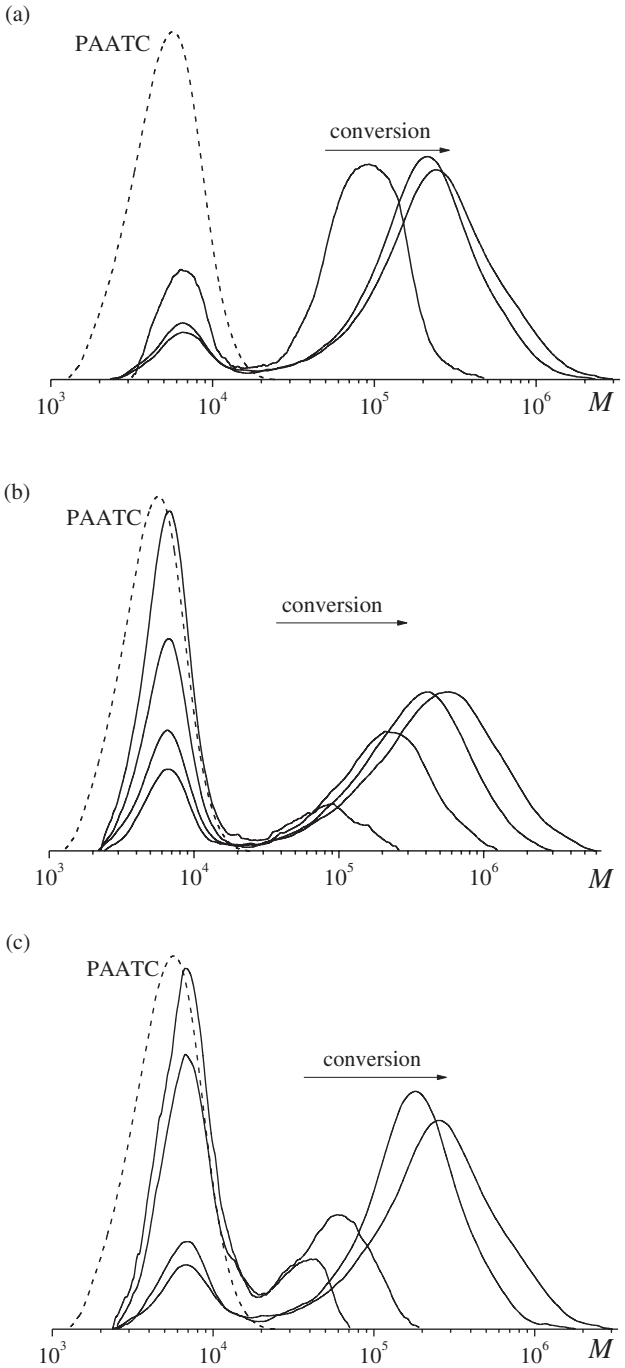

Figure 6. SEC curves normalized to unit area for the polymers formed at various monomer conversions during the batch emulsion polymerization of BA at 70 °C mediated by 10 wt% PAATC, water:monomer = 10:1 v/v, for a concentration of PSK of (a) 1 wt%, (b) 0.9 wt% and (c) 0.75 wt%.

The semi-batch regime of emulsion polymerization has no effect on the evolution of the MWD with monomer conversion: a bimodal shape of the MWD is observed for both co-monomers HFBA (Fig. 11(a)) and OFPA (Fig. 11(b)). An increase in concentration of PSK leads to additional broadening of the maximum in the MWD corresponding to the fraction of high molecular weight product (Fig. 11(c)).

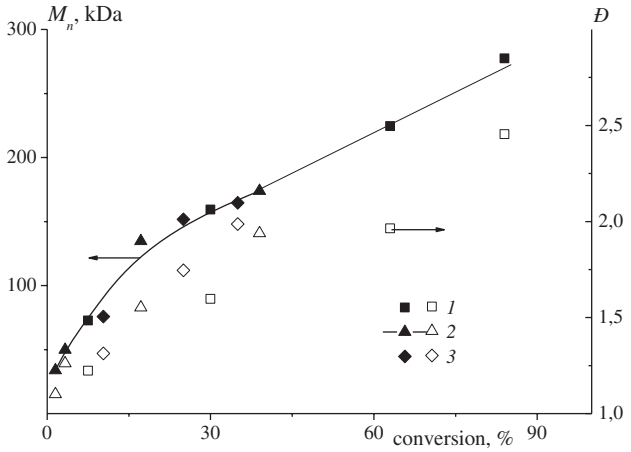

Figure 7. Dependence of M_n and $Đ$ on monomer conversion for the high molecular 'grown' polymers formed during the batch emulsion polymerization of BA at 70 °C mediated by 10 wt% PAATC, water:monomer = 10:1 v/v, for a concentration of PSK of 1 wt% (points 1), 0.9 wt% (points 2) and 0.75 wt% (points 3).

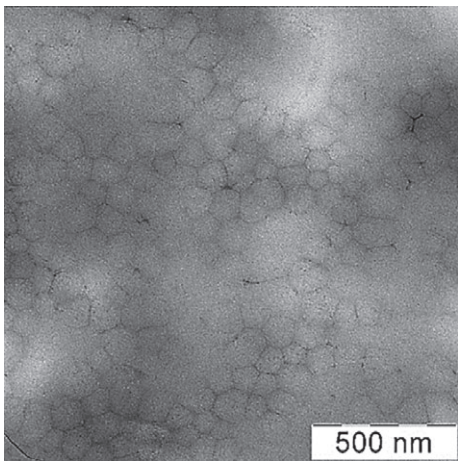

Figure 8. TEM image of the thin film formed from the dispersion produced by the emulsion polymerization of BA in the presence of PAATC; water:monomer = 10:1 v/v.

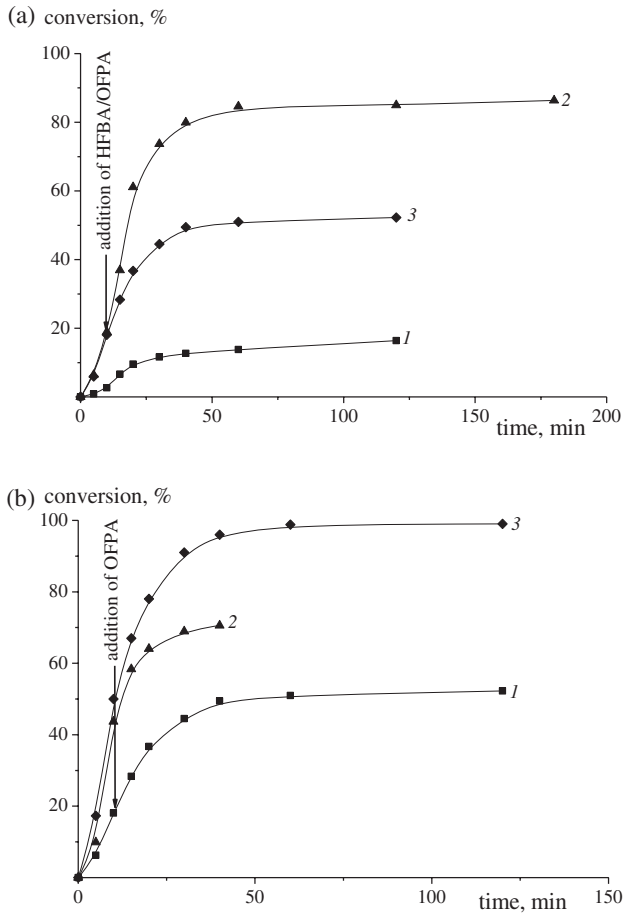

Figure 9. Dependence of monomer conversion on the reaction time for the emulsion copolymerization of BA and fluoroalkyl acrylates at 70 °C in the presence of 10 wt% PAATC, water:monomers = 10:1 v/v, [BA]/[HFBA] = [BA]/[OFPA] = 80/20 mol mol^{-1}: (a) 1 wt% of PSK, monomer HFBA (curves 1 and 2) and OFPA (curve 3), batch regime curve 1 and semi-batch regime curves 2 and 3; (b) monomer OFPA, semi-batch regime, PSK content 1 wt% (curve 1), 1.5 wt% (curve 2) and 2 wt% (curve 3).

As expected, the semi-batch regime has no effect on the morphology of the particles because both copolymerization systems exhibit similar kinetic features, as described above for batch emulsion polymerization. Typical TEM micrographs of thin films obtained from the dispersions after completion of polymerization are presented in Fig. 12. As seen from the figure, spherical particles with sharp edges and an average diameter similar to that determined by DLS are observed.

Summarizing, we conclude that independently of the polymerization conditions the emulsion homopolymerization and copolymerization of BA mediated by PAA containing the trithiocarbonate group in the chain results in the synthesis of polymers with a bimodal MWD. These polymers form a stable dispersion *in situ* of particles of spherical morphology with the core–shell structure. As a plausible hypothesis, we suppose that the low molecular weight fraction corresponds to the block copolymer with a short hydrophobic block, while the high molecular weight fraction comprises block copolymers with a long hydrophobic block, the length of which is about two orders of magnitude longer than that of the hydrophilic block, and the homopolymer of BA. In this case, the core of the particles comprises both BA blocks of the block copolymer and poly(BA) chains. In the following section, we use simple theoretical arguments for analysis of the effect of the presence of the homopolymer in the core on the shape of the core–shell particles.

Morphology of core–shell–corona nanoaggregates: a theoretical model

Here we consider nanoaggregates formed upon co-assembly of amphiphilic diblock copolymers (N_A and N_B being the degrees of polymerization of the hydrophilic and hydrophobic blocks, respectively) and 'droplets' formed by long hydrophobic polymers chemically identical to blocks B phase separated from aqueous solution. We note that, since both A and B blocks in such aggregates are stretched, our results apply with good accuracy to a system comprising, instead of a diblock, a triblock copolymer ABA with a doubled length of the central B block. Block copolymers stabilize droplets of homopolymer B against aggregation by forming a layer at the droplet–water interface with B blocks constituting a dry (solvent free) shell and A chains protruding into the aqueous phase and forming a solvated corona (Fig. 13). We consider the case when homopolymer B chains are sufficiently

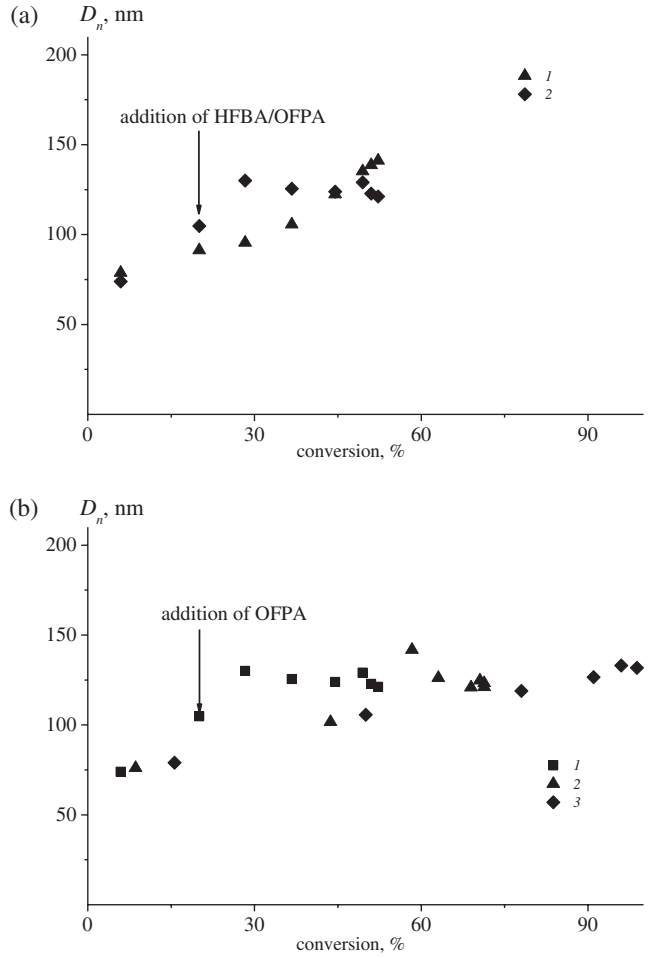

Figure 10. Dependence of the number-average diameter D_n of the particles on polymerization time for semi-batch emulsion copolymerization of BA and fluoroalkyl acrylates at 70 °C in the presence of 10 wt% PAATC, water:monomers = 10:1 v/v, [BA]/[HFBA] = [BA]/[OFPA] = 80/20 mol mol^{-1}: (a) 1 wt% of PSK, monomer HFBA (points 1) and OFPA (points 2); (b) OFPA, PSK content 1 wt% (points 1), 1.5 wt% (points 2) and 2 wt% (points 3).

long and do not penetrate into the shell formed by stretched B blocks.

We aim to analyze how the size of the inner core comprising the hydrophobic B homopolymer affects the morphologies of the core–shell–corona aggregates, i.e. to establish parameter ranges corresponding to thermodynamic stability of spherical *versus* cylindrical aggregates.

The free energy of an aggregate of arbitrary morphology (calculated per one block copolymer chain) can be presented as the sum of three contributions:

$$F^{(i)}(s) = F^{(i)}_{\text{shell}}(s) + F^{(i)}_{\text{surf}}(s) + F^{(i)}_{\text{corona}}(s) \quad (1)$$

where s is the area per block copolymer molecule at the B shell–A corona interface and i = 1, 2, 3 refers to spheres, cylinders and lamellae, respectively. The respective contributions to the free energy in Eqn (1) account for the conformational entropy of extended B blocks in the shell, the excess free energy of the shell–corona interface and conformational entropy and excluded volume interactions of solvated A blocks in the corona domain. Assuming good solvent conditions for soluble blocks A we can

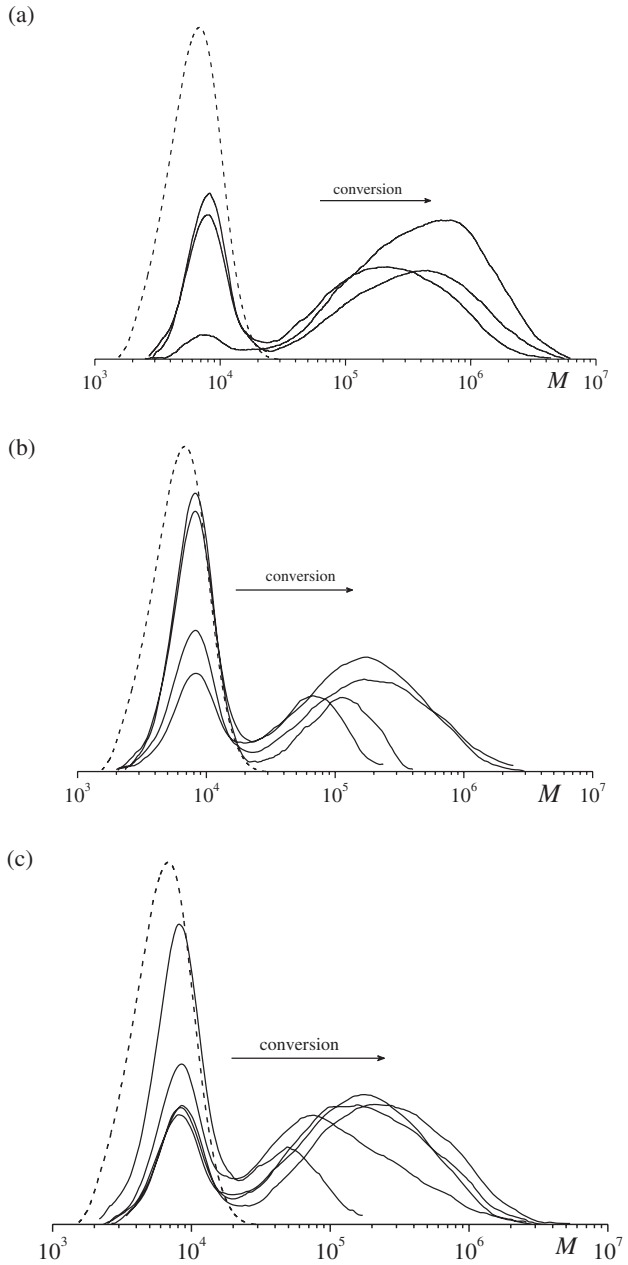

Figure 11. SEC curves normalized to unit area for polymers formed at various monomer conversions during semi-batch emulsion copolymerization of BA and fluoroalkyl acrylates at 70 °C in the presence of 10 wt% PAATC, water:monomers = 10:1 v/v, [BA]/[HFBA] = [BA]/[OFPA] = 80/20 mol mol^{-1}: (a) HFBA, 1 wt% PSK; (b) OFPA, 1 wt% PSK; (c) OFPA, 1.5 wt% PSK.

present the free energy of the corona (in a mean-field approximation, following Zhulina and Borisov[8]) as

$$F^{(i)}_{\text{corona}}(s) = F^{(1)}_{\text{corona}}(s)\left[1 + \frac{1-i}{3}\frac{D^{(1)}}{R}\right] \quad (2)$$

where R is the radius of curvature of the B shell–A corona interface and

$$F^{(1)}_{\text{corona}}(s) = \frac{3^{1/3}}{2} N_A v^{2/3} \left(\frac{s}{a^2}\right)^{-2/3}$$
$$D^{(1)} = \frac{1}{3^{1/3}} N_A v^{1/3} \left(\frac{s}{a^2}\right)^{-1/3} \quad (3)$$

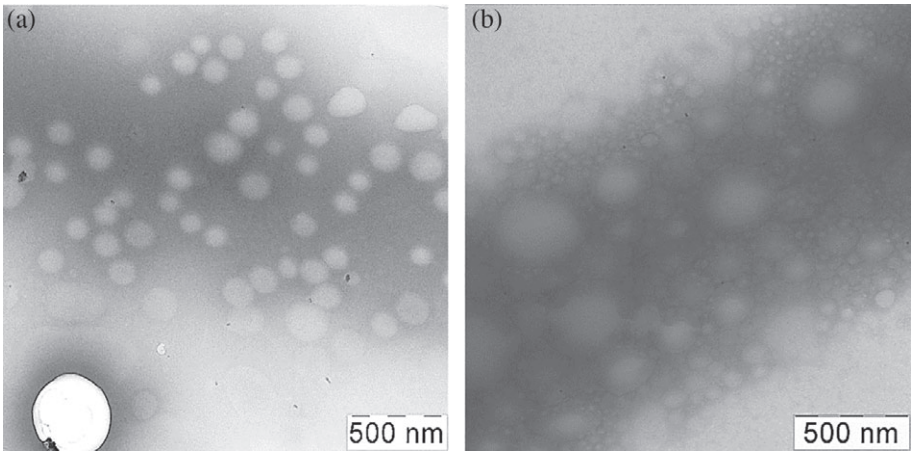

Figure 12. TEM image of the thin films formed from the dispersion produced by the semi-batch emulsion copolymerization of BA and fluoroalkyl acrylates at 70 °C in the presence of 10 wt% PAATC and 1 wt% of PSK, water:monomers = 10:1 v/v, [BA]/[HFBA] = [BA]/[OFPA] = 80/20 mol mol^{-1}: (a) HFBA; (b) OFPA.

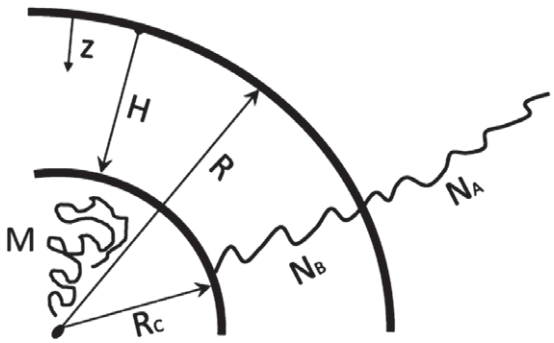

Figure 13. Schematic presentation of a core–shell nanoparticle formed by an AB block copolymer and homopolymer B. N_A and N_B are the degrees of polymerization of the hydrophilic, (A) and hydrophobic (B) blocks, respectively. M is the total number of monomer units in homopolymer chain(s) per one block copolymer. R_c is the radius of the central core formed by homopolymers. R is the outer radius of the insoluble shell formed by B blocks of the block copolymers and H is the thickness of this shell.

are, respectively, the free energy and the thickness of a brush formed by A chains tethered to the planar interface between the B shell and solvent (in the limit $R \to \infty$) and the second term in Eqn (2) is the first-order correction in powers of reduced curvature D/R. Here $v > 0$ is the second virial coefficient (excluded volume parameter) for A monomer units; all lengths are measured in the monomer unit length a whereas all energy values are expressed in units of thermal energy $k_B T$.

The excess free energy of the interface between the dry B shell and water can be presented as

$$F_{surf}(s) = \gamma s(R)\, a^{-2} \tag{4}$$

where γ is the dimensionless surface tension and

$$s(R_i) = \frac{i(N_B + M)}{\varphi R_i} \tag{5}$$

is the area of the interface per one block copolymer chain with M being the number of B monomers in the core per one block copolymer. Equation (5) follows from the condition of a uniform volume fraction φ of monomer units B in both the core domain formed by homopolymer B and the shell domain formed by B blocks of the diblock copolymers.

By minimizing the free energy Eqn (1) with respect to $s(R)$ we find the equilibrium surface area per chain:

$$\frac{\partial F}{\partial s} = 0 \to s = 3^{1/5}\left(\frac{N_A}{\gamma}\right)^{3/5} v^{2/5} a^2 \tag{6}$$

which in a first approximation is the same in the aggregates of any morphology as long as we account only for the balance of the leading terms in Eqn (1), i.e. $F^{(1)}_{corona}(s) + F_{surf}(s)$.

The binodal line corresponding to coexistence of aggregates of morphologies i and $i+1$ is found from the condition $F^{(i)}(s) = F^{(i+1)}(s)$, which leads to

$$F^{(i)}_{shell}(s) + \frac{1-i}{3}\frac{F^{(1)}_{corona}(s)\, D^{(1)}}{R_{(i)}(s)} = F^{(i+1)}_{shell}(s) + \frac{(-i)}{3}\frac{F^{(1)}_{corona}(s)\, D^{(1)}}{R_{(i+1)}(s)} \tag{7}$$

or, taking into account Eqns (3) and (5),

$$F^{(i+1)}_{shell}(s) - F^{(i)}_{shell}(s) = \frac{1}{2i(i+1)}\frac{N_A^2 v\varphi}{N_B + M} \tag{8}$$

The conformational free energy of the stretched B blocks in the shell can be calculated as

$$F_{shell}(z) = \int_0^H f_{elast}(z)\, s(z)\, dz \tag{9}$$

where

$$f_{elast}(z) = \frac{1}{s(z)}\frac{3\pi^2}{8N_B^2 a^2}\int_z^H z' s\left(z'\right)\varphi\left(z'\right) dz' \tag{10}$$

is the density of the elastic free energy and H is the thickness of the shell (see Fig. 14),

$$s(z) = s(R)\left(\frac{R-z}{R}\right)^{i-1} \tag{11}$$

and $0 < z < H$. Under the conditions of a constant density of the shell

$$\varphi\left(z'\right) \equiv \varphi \tag{12}$$

and finally we obtain

$$F_{\text{shell}}(Z) = \frac{3\pi^2}{8N_B^2a^2}\frac{i\left(N_B+M\right)}{\varphi R}\int_0^H z'^2\left(\frac{R-z'}{R}\right)^{i-1}\mathrm{d}z'$$

$$i = 1,\ 2,\ 3 \qquad (13)$$

From packing conditions the thickness of the shell is

$H_i = R_i\left[1-\left(1+\frac{N_B}{M}\right)^{-1/i}\right]$

Then the conformational free energy of the B shell is given by

$$F_{\text{shell}}^{(2)} = \frac{\pi^2}{16N_B^2a^2}\frac{M+N_B}{R_{(2)}^2}\left(4H_{(2)}^3R_{(2)}-3H_{(2)}^4\right) \qquad (14)$$

in the cylindrical case ($i = 2$) and

$$F_{\text{shell}}^{(3)} = \frac{3\pi^2}{80N_B^2a^2}\frac{M+N_B}{R_{(3)}^3}\left(10R_{(3)}^2H_{(3)}^3-15H_{(3)}^4R_{(3)}+6H_{(3)}^5\right) \qquad (15)$$

in the spherical case ($i = 3$).

We introduce the notation $x = M/N_B$ and the geometry-dependent function

$$I_i(x) = \left[1-\left(1+\frac{N_B}{M}\right)^{-1/i}\right] = \left[1-\left(\frac{x}{x+1}\right)^{1/i}\right] \qquad (16)$$

Taking account of these notations, Eqns (14) and (15) can be rewritten as follows.

Cylindrical case:

$$F_{\text{shell}}^{(2)} = \frac{\pi^2N_B}{\varphi^2s^2a^{-4}}(x+1)^3I_{(2)}^3(x)\left[1-\frac{3}{4}I_{(2)}(x)\right] \qquad (17)$$

Spherical case:

$$F_{\text{shell}}^{(3)} = \frac{3^4\pi^2N_B}{2^3\varphi^2s^2a^{-4}}(x+1)^3I_{(3)}^3(x)\left[\frac{1}{3}-\frac{1}{2}I_{(3)}(x)+\frac{1}{5}I_{(3)}^2(x)\right] \qquad (18)$$

Then the binodal line for the sphere–cylinder transition can be presented as

$$\frac{\pi^2N_B}{\varphi^2s^2a^2}(x+1)^3\left\{\frac{3^4}{2^3}I_{(3)}^3(x)\left[\frac{1}{3}-\frac{1}{2}I_{(3)}(x)+\frac{1}{5}I_{(3)}^2(x)\right]\right.$$

$$\left.-I_{(2)}^3(x)\left[1-\frac{3}{4}I_{(2)}(x)\right]\right\} = \frac{1}{12}\frac{N_A^2v\varphi}{N_B(1+x)} \qquad (19)$$

or

$$\frac{12\pi^2N_B^2}{a^2\varphi^2s^2N_A^2v\varphi}(x+1)^4\left\{\frac{3^4}{2^3}I_{(3)}^3(x)\left[\frac{1}{3}-\frac{1}{2}I_{(3)}(x)+\frac{1}{5}I_{(3)}^2(x)\right]\right.$$

$$\left.-I_{(2)}^3(x)\left[1-\frac{3}{4}I_{(2)}(x)\right]\right\} = 1 \qquad (20)$$

We further introduce the function

$$G(x) = (x+1)^4\left\{\frac{3^4}{2^3}I_{(3)}^3(x)\left[\frac{1}{3}-\frac{1}{2}I_{(3)}(x)+\frac{1}{5}I_{(3)}^2(x)\right]\right.$$

$$\left.-I_{(2)}^3(x)\left[1-\frac{3}{4}I_{(2)}(x)\right]\right\} \qquad (21)$$

$$G(0) = 0.0875$$

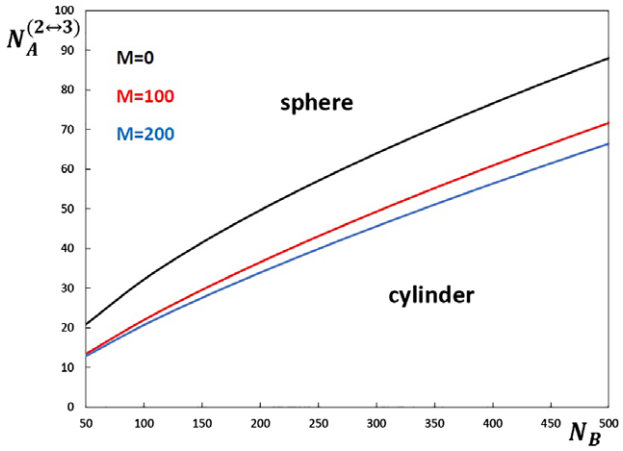

Figure 14. Binodal lines separating regions of thermodynamic stability of spherical and cylindrical core–shell–corona nanoparticles at different numbers M of hydrophobic monomer units in the core. The black line ($M = 0$) corresponds to coexistence between spherical and cylindrical micelles formed by the pure block copolymer AB.

Finally the equation for the binodal line separating ranges of thermodynamic stability of spherical and cylindrical aggregates can be written as

$$N_B^{(2\leftrightarrow3)} = \frac{\varphi^{3/2}N_A^{8/5}v^{9/10}}{3^{3/10}*2\pi\gamma^{3/5}}\frac{1}{\sqrt{G(x)}} \qquad (22)$$

Obviously, at $x = 0$ we recover the binodal line for the sphere to cylinder transition in a pure AB diblock copolymer micelle. An increase in x, i.e. an increase in the size of the inner B core, leads to a shift of the transition from spheres to cylinders to larger N_B.

Equation (22) can be rewritten as

$$N_A^{(2\leftrightarrow3)} = \left[2\pi3^{3/10}\sqrt{G(x)}\right]^{5/8}\left(\gamma^{3/8}/v^{9/16}\varphi^{15/16}\right)N_B^{5/8} \qquad (23)$$

In Fig. 14, $N_A^{(2\leftrightarrow3)}\left(N_B\right)$ is plotted according to Eqn (23) for $x = 0$ ($M = 0$, sphere to cylinder binodal for the pure block copolymer system) and for selected values of $M = 100, 200, \ldots$ (setting $\gamma = 1$, $v = 1$, $\varphi = 1$). We see that upon increase in M the binodal line separating ranges of stability of spherical and cylindrical aggregates is shifted down towards larger values of N_B (smaller values of N_A).

Hence, block copolymers that form cylindrical micelles alone are capable of spherical particle formation if the core size is large enough. In other words, an increase in the core size stabilizes the spherical morphology of the aggregates even when the block copolymers alone form cylindrical wormlike micelles.

CONCLUSIONS

The results of our studies have revealed the unusual behavior of macroRAFT agents based on symmetrical trithiocarbonates in emulsifier-free emulsion polymerization. We anticipate that this specific property of the macroRAFT agent can be explained by the locus of the trithiocarbonate group in the middle of the chain. In contrast to solution and dispersion polymerization, emulsion polymerization leads to a polymeric product which is characterized by a bimodal MWD. This result is achieved irrespective of the chemical nature of the PAA-based macroRAFT agent

with trithiocarbonate group located within the chain and polymerization conditions that include the chemical nature of the initiator, the molar ratio of initiator to macroRAFT agent, the volume ratio of water to monomer, monomer addition regime etc.

We suppose that the low molecular weight fraction consists of block copolymers with a short hydrophobic block. The high molecular fraction may consist of block copolymers with a long hydrophobic block, which exceeds the hydrophilic block by at least two orders of magnitude, and a certain amount of hydrophobic homopolymer (or copolymer when a mixture of hydrophobic monomers is used). This apparent violation of the RAFT polymerization mechanism may be due to restricted access of the trithiocarbonate group in the block copolymer with short hydrophobic block for propagating radicals that penetrate into the particle. As a result, most of the macromolecules with short hydrophobic block serve as stabilizers of the particles rather than macroRAFT agents. Additionally, in this case, polymeric particles formed in the course of emulsion polymerization reveal only spherical morphologies.

We have used mean-field theoretical arguments to prove that the presence of insoluble homopolymer chains or block copolymers with negligibly short hydrophilic blocks in the core leads to extension of the thermodynamic stability range of spherical aggregates that correlates with our experimental observation.

ACKNOWLEDGEMENTS

This research was financially supported by the Russian Foundation for Basic Research (project no. 16-53-76007, part of the Joint Project ERA.Net RUS Plus: SAS-MEM 254, project no. 18-33-00386 and project no. 17-03-00131). We are grateful to S. S. Abramchuk (Moscow State University) for assistance in TEM analysis.

DATA AVAILABILITY

The raw/processed data required to reproduce these findings cannot be shared at this time as the data also forms part of an ongoing study.

REFERENCES

1 Mai Y and Eisenberg A, *Chem Soc Rev* **41**:5969–5985 (2012).
2 Lazzari M, Lin G and Lecommandoux S, *Block Copolymers in Nanoscience*. Wiley-VCH, Weinheim (2006).
3 Schacher FH, Rupar PA and Manners I, *Angew Chem Int Ed* **51**:7898–7921 (2012).
4 Hadjichristidis N, Pispas S and Floudas G, *Block Copolymers: Synthetic Strategies, Physical Properties, and Applications*. John Wiley & Sons, Hoboken, NJ (2003).
5 Honda C, Hasegawa Y, Hirunuma R and Nose T, *Macromolecules* **27**:7660–7668 (1994).
6 Reiss G, *Prog Polym Sci* **28**:1107–1170 (2003).
7 Moffitt M, Khougaz K and Eisenberg A, *Acc Chem Res* **29**:95–102 (1996).
8 Zhulina EB and Borisov OV, *Macromolecules* **45**:4429–4440 (2012).
9 Zhang L and Eisenberg A, *J Am Chem Soc* **118**:3168–3181 (1996).
10 Borisov OV and Zhulina EB, *Macromolecules* **36**:10029–10036 (2003).
11 Zhulina EB, Adam M, Sheiko SS, LaRue I and Rubinstein M, *Macromolecules* **38**:5330–5351 (2005).
12 Borisov OV, Zhulina EB, Leermakers FAM and Müller AHE, *Adv Polym Sci* **241**:57–129 (2011).
13 Lansalot M, Rieger J and D'Agosto F, Polymerization-induced self-assembly: the contribution of controlled radical polymerization to the formation of self-stabilized polymer particles of various morphologies, in *Macromolecular Self-Assembly*, ed. by Billon L and Borisov O. John Wiley and Sons, Inc., Hoboken, NJ, pp. 33–82 (2016).
14 Canning SL, Smith GN and Armes SP, *Macromolecules* **49**:1985–2001 (2016).
15 Charleux B, Delaittre G, Rieger J and D'Agosto F, *Macromolecules* **45**:6753–6765 (2012).
16 Charleux B, Monteiro MJ and Heuts H, Living radical polymerisation in emulsion and miniemulsion, in *Chemistry and Technology of Emulsion Polymerisation*, ed. by van Herk AM. Blackwell Publishing Ltd, Oxford, UK, pp. 105–143 (2013).
17 Zetterlund PB, Kagawa Y and Okubo M, *Chem Rev* **108**:3747–3794 (2008).
18 Zhang X, Rieger J and Charleux B, *Polym Chem* **3**:1502–1509 (2012).
19 Zhang W, D'Agosto F, Boyron O, Rieger J and Charleux B, *Macromolecules* **45**:4075–4084 (2012).
20 Müller AHE and Matyjaszewski K, *Controlled and Living Polymerizations: Methods and Materials*. Wiley-VCH, Verlag GmbH & Co. KGaA, Weinheim (2009).
21 Matyjaszewski K, Sumerlin BS and Tsarevsky NV, *Progress in Controlled Radical Polymerization: Materials and Applications*. American Chemical Society, Washington, DC (2012). (ACS Symposium Series, 1101).
22 Matyjaszewski K, Sumerlin BS, Tsarevsky NV and Chiefari J, *Controlled Radical Polymerization: Mechanisms*. American Chemical Society, Washington, DC (2015) (ACS Symposium Series, 1187).
23 Moad G, Rizzardo E and Thang SH, *Aust J Chem* **65**:985–1076 (2012).
24 Moad G, Rizzardo E and Thang SH, *Polymer* **49**:1079–1131 (2008).
25 Boyer C, Stenzel MH and Davis TP, *J Polym Sci Polym Chem* **49**:551–595 (2011).
26 Chernikova EV and Sivtsov EV, *Polym Sci Ser B* **59**:117–146 (2017).
27 Derry MJ, Fielding LA and Armes SP, *Polym Chem* **6**:3054–3062 (2015).
28 Zhang W, D'Agosto F, Boyron O, Rieger J and Charleux B, *Macromolecules* **44**:7584–7593 (2011).
29 Chernikova EV, Plutalova AV, Mineeva KO, Nasimova IR, Kozhunova EY, Bol'shakova AV *et al.*, *Polym Sci Ser B* **57**:547–559 (2015).
30 Chernikova EV, Serkhacheva NS, Smirnov OI, Prokopov NI, Plutalova AV, Lysenko EA *et al.*, *Polym Sci Ser B* **58**:629–639 (2016).
31 Serkhacheva NS, Smirnov OI, Tolkachev AV, Prokopov NI, Plutalova AV, Chernikova EV *et al.*, *RSC Adv* **7**:24522–24536 (2017).
32 Serkhacheva NS, Plutalova AV, Kozhunova EY, Prokopov NI and Chernikova EV, *Polym Sci Ser B* **60**:204–217 (2018).
33 Chenal M, Bouteiller L and Rieger J, *Polym Chem* **4**:752–762 (2013).
34 Chaduc I, Crepet A, Boyron O, Charleux B, D'Agosto F and Lansalot M, *Macromolecules* **45**:5881–5891 (2012).
35 Chernikova EV, Terpugova PS, Garina ES and Golubev VB, *Polym Sci Ser A* **49**:108–119 (2007).
36 Moad G, Rizzardo E and Thang SH, *Polym Int* **60**:9–25 (2011).
37 Chernikova EV, Plutalova AV, Garina ES and Vishnevetsky DV, *Polym Chem* **7**:3622–3632 (2016).

